PENSOFT.

SENCKENBERG
world of biodiversity

Leibniz
Association

The first fossil Hybocephalini (Coleoptera: Staphylinidae: Pselaphinae) from the middle Eocene of Europe and its evolutionary and biogeographic implications

Zi-Wei Yin[1], Erik Tihelka[2,3], Jesus Lozano-Fernandez[4], Chen-Yang Cai[2,3]

1   *Laboratory of Systematic Entomology, College of Life and Environmental Sciences, Shanghai Normal University, Shanghai, 200234, China*

2   *State Key Laboratory of Palaeobiology and Stratigraphy, Nanjing Institute of Geology and Palaeontology, and Center for Excellence in Life and Paleoenvironment, Chinese Academy of Sciences, Nanjing 210008, China; cycai@nigpas.ac.cn*

3   *School of Earth Sciences, University of Bristol, Life Sciences Building, Tyndall Avenue, Bristol, BS8 1TQ, UK*

4   *Department of Genetics, Microbiology and Statistics, Biodiversity Research Institute (IRBio), University of Barcelona, Avd. Diagonal 643, 08028*

http://zoobank.org/urn:lsid:zoobank.org:pub:1D57CB0C-56C4-4DA5-91E1-CF7E9BB40E74

Corresponding author: Zi-Wei Yin (pselaphinae@gmail.com)

Citation: Yin Z-W, Tihelka E, Lozano-Fernandez J, Cai C-Y (2022) The first fossil Hybocephalini (Coleoptera: Staphylinidae: Pselaphinae) from the middle Eocene of Europe and its evolutionary and biogeographic implications. Arthropod Systematics & Phylogeny 80: 279–294. https://doi.org/10.3897/asp.80.e82644

Abstract

The extant tropical tribe Hybocephalini is a morphologically highly derived group of the subfamily Pselaphinae (Coleoptera: Staphylinidae), which is characterized most notably by the modified squamous setae that cover various parts of the body. Ten genera and 69 extant species have been found in the Afrotropical and Oriental regions, with one species found in northern Australia. Prior to this study the evolutionary history of the tribe has been remained elusive due to the dearth of known fossils. Here, we describe the first fossil representative of Hybocephalini, *Europharinodes schaufussi* Yin & Cai **gen. et sp. nov.**, based on an adult male preserved in Baltic amber (*ca* 45.0–38.0 Ma). Using X-ray microtomography, the anatomy including the endoskeletal structures of the head, the full pattern of foveation, and the aedeagus of the beetle were reconstructed. *Europharinodes* shares most derived traits that are congruent with extant members of Hybocephalini, but it also possesses plesiomorphic and autapomorphic characters unknown in living relatives. In order to constrain the phylogenetic placement of *Europharinodes*, we created an updated morphological character matrix to explore relationships among this genus and related groups. A monophyletic Hybocephalini was recovered by maximum likelihood and parsimony analyses, with *Europharinodes* being well-resolved as sister to all modern relatives in the likelihood tree. The fossil thus sheds new light on the morphological evolution of Hybocephalini and suggests a broader palaeodistribution of the tribe during the middle Eocene. The disjunct distribution of an Eocene Baltic amber species and an extant Afrotropical-Oriental distribution of the tribe is probably relictual, and was shaped by global cooling during the Eocene–Oligocene transition.

Keywords

1.   Introduction

Comprising more than 64,000 extant and 400 extinct species, the Staphylinidae (rove beetles) stands for the most species-rich family in the whole animal kingdom, surpassing Curculionidae (true weevils) (Yin et al. 2020; Shin et al. 2017). Among the 32 currently recognized extant subfamilies of Staphylinidae, the Pselaphinae are the second most diverse lineage (following Aleocharinae) containing over 10,000 extant species classified in 40 tribes and 1,259 described genera worldwide (Newton and Chandler 1989; Yin et al. 2019a), albeit this perhaps represents only a small fraction of their true diversity (Löbl and Kurbatov 2001; Yin 2022).

Six supertribes of Pselaphinae have been recognized and are applied to current taxonomic practice (Newton and Thayer 1995; Chandler 2001): the basal-most Faronitae, and its sister clade including the other five supertribes (Euplectitae, Goniaceritae, Batrisitae, Pselaphitae, Clavigeritae) forming the so-called 'higher Pselaphinae' (Parker 2016). The phylogenetic relationships among these supertribes, except for the position of Faronitae, remains unstable because most of them and many included large tribes (e.g., Trichonychini) were shown to be paraphyletic in recent taxonomic or phylogenetic studies (e.g., Chandler 2001; Parker 2016; Jałoszyński et al. 2022). This poor state of knowledge is further exacerbated by a paucity of direct (fossil) evidence pertaining to the evolutionary history of major pselaphine groups. The research of the fossil history of pselaphines experienced two stages. The first stage lasted from the 1890s to the 1920s (for a review of taxa see Spahr 1981; Newton and Chandler 1989), during which Schaufuss (1890) described a diverse pselaphine fauna from the middle Eocene Baltic amber. The Baltic Pselaphinae, like most other insect groups (Weitschat and Wichard 2010), shows affinities to extant lineages, thus providing little information on how and when the higher lineages may have originated. Furthermore, meaningful re-interpretations of this fauna become almost impossible because of Schaufuss' limited species descriptions usual for his time, and the fact that his type materials were lost during World War II. A second surge of interest in fossil Pselaphinae started only recently, tracking an increasing discovery of the Mesozoic amber inclusions originating from northern Myanmar (Ross 2019–2021). Several stem-group members of Euplectitae and Goniaceritae were described from this deposit (Parker 2016; Yin et al. 2017; 2019a, b, 2021; Yin and Cai 2021), which shed new light on the paleobiogeography and certain trends in morphological evolution within these two supertribes. Not long ago, a critical fossil representative of stem-group Clavigeritae, *Protoclaviger trichodens* Parker and Grimaldi, was described (Parker and Grimaldi 2014) from the Ypresian Cambay amber (Rust et al. 2010) of western India, which shows a transitional body form foreshadowing the extreme myrmecophily of recent clavigerites before the rise of modern ants.

The tribe Hybocephalini is a morphologically highly derived group of the supertribe Pselaphitae, characterized most remarkably by the presence of squamous setae that cover various parts of the body, combined with its dorsoventrally convex body, and greatly transverse antennomeres (Nomura 1989; Chandler 2001; Yin and Jiang 2017). To date ten genera and 69 extant species have been described from the Afrotropical and Oriental regions (Newton 2018), with one species of these genera found in northern Australia (Chandler 2001). All species of Hybocephalini are relatively rarely encountered in the field. They are collected from leaf litter samples (Nomura 1991a; Sugaya 2003), from under stones (Yin and Jiang 2017), by flight intercept traps, or more often, attracted by ultraviolet light traps (e.g., Jeannel 1950; Chandler 2001). *Apharinodes sinensis* Yin & Jiang was found to exhibit male wing dimorphism (Yin and Jiang 2017), suggesting complex trade-offs may exist during the life history of this species. Prior to the present study no fossil representatives of Hybocephalini have been known, complicating attempts at disentangling the evolutionary history of this tribe. Here, the first fossil hybocephaline, *Europharinodes* **gen. nov.**, is described from the middle Eocene Baltic amber. Aided by X-ray microtomography, the fine anatomy of the beetle has been reconstructed, including the endoskeletal structures of the head. An updated morphological character matrix was constructed to further determine the placement of the fossil, and the biogeographic implications of the new findings are discussed. *Europharinodes* represents the first extinct Pselaphitae described in detail since the century-old Schaufuss species descriptions.

2.   Material and methods

2.1.   Location, age and processing of the amber

The Baltic amber (Figs 2–5) studied here was collected at the Yantarny settlement, Sambian Peninsula, Kaliningrad Oblast, Russia (54°52'N, 19°58'E). The age of Baltic amber follows that discussed in Bukejs et al. (2019), dated as 45.0–38.0 Ma (Bartonian to Priabonian, mid-late Eocene). The material is deposited in the Insect Collection of the Shanghai Normal University (SNUC), under the accession number 'SNUC-Paleo-0102'. The amber piece was cut using a handheld rotary tool equipped with a diamond blade, ground with sandpapers of different grain sizes, and then polished with rare earth polishing powder. The base map (Fig. 6A) showing the palaeolocation of the amber forest was retrieved from Poblete et al. (2021), indicating an age of 40 Ma. The distribution map of recent Hybocephalini (Fig. 6B) was created using QGIS 3.10.8, with the base map acquired from the Web Map Service at https://www.simplemappr.net (Shorthouse 2010). The distributions of a majority of modern species were estimated from published literature, usually with only the country/region known. Since many of the distribution spots are identical, extant species density of

the tribe is shown and was estimated by the 'heatmap renderer' function (Kernel Density Estimation) of QGIS.

2.2. Fossil imaging and 3-D reconstruction

Photographs under incident light were taken using a Canon 5D Mark III camera equipped with a Canon MP-E 65 mm macro lens (Figs 2B; 3A), with an attached Canon MT-24EX twin flash as the light source; or using a Canon G9 camera mounted on an Olympus CX31 microscope (Figs 2G; 3C, D, I). Zerene Stacker Version 1.04 was used for image stacking. Using the same method as Li et al. (2021), the amber inclusion was imaged using high-resolution X-ray microtomography (micro-CT) to uncover fine morphological detail. Scans were made using a Zeiss Xradia 520 versa at the micro-CT laboratory of the Nanjing Institute of Geology and Palaeontology, CAS. A CCD-based 4× objective was used, providing isotropic voxel sizes of 2.6365 µm with the help of geometric magnification. During the scanning, the acceleration voltage of the X-ray source was 40 kV. To improve the signal-to-noise ratio, 992 projections over 360° were collected, and the exposure time for each projection was 2 s. The tomographic data were analyzed using Avizon ver. 2019.1. An Isosurface threshold value between 15.000 and 17.500 was used. Images were further processed and arranged into plates in Adobe Photoshop CC ver. 20.0.1.

2.3. Phylogenetic analysis

To test the phylogenetic position of the new fossil taxon within Pselaphinae, we incorporated the new material into previously published datasets (Parker 2016; Yin et al. 2017, 2019b). In addition to *Apharinodes papageno* Nomura, which was included in the original dataset, we added four more taxa belonging to the genera of Hybocephalini to expand focus on the tribe. A newly described fossil of the tribe Brachyglutini (Yin et al. 2019a) was also included, adding up to 58 non-additive and unordered adult morphological characters coded for 63 taxa (Supplementary material 1). Inapplicable character states are indicated by 'en' dashes (–), and missing data are indicated by question marks (?). The data matrix (Supplementary material 2) was assembled in WinClada 1.00.08 (Nixon 2002); characters are numbered starting from 1.

Maximum likelihood (ML) analysis was performed using IQ-TREE v. 2.1.3 (Nguyen et al. 2015) with a single partition. The Mk+FQ+ASC+G4 model was selected as the best-fitting model by the built-in program ModelFinder (Kalyaanamoorthy et al. 2017). Branch support values were estimated by 1,000 duplications of ultrafast bootstraps. Ten independent runs were executed and the result with the highest likelihood was selected as the best ML tree. Bayesian analysis was performed using MrBayes 3.2.6 (Ronquist et al. 2012) under the Mk model with Gamma distributed rates (Lewis 2001; Yang 1994).

The search consisted of two Markov chain Monte Carlo (MCMC) runs of two chains and was terminated at ten million generations. Convergence was determined by the standard deviation of split frequencies having dropped below 0.0075, and further verified by estimated sample sizes higher than 200 in Tracer v1.7.1 (Rambaut et al. 2018), indicating sufficient estimation of the posterior values. The first 25% of trees were discarded as burn-in. Both maximum likelihood and Bayesian analyses were rooted on *Scirtes hemisphericus*. Clades with bootstrap values of 95–100% were considered to be strongly supported, 80–94% moderately supported, and 50–79% weakly supported (Hoang et al. 2018). Maximum parsimony (MP) analysis (Supplementary material 3) was conducted in TNT v1.5 (Goloboff and Catalano 2016) under implied weighting (default weighting function K = 3) using the 'Traditional search' strategy; the collapsing rule was switched to 'none'. Standard Bootstrap value was also calculated in TNT. Character mapping on the consensus tree was made in WinClada 1.00.08 (Nixon 2002). The trees shown in the text (Fig. 1) were annotated in FigTree v1.4.3 (http://tree.bio.ed.ac.uk/software/figtree), and graphically edited using Adobe Illustrator CS5.

3. Results

3.1. Phylogenetic analyses

To test the placement of the new fossil taxon with Pselaphinae, both maximum likelihood and parsimony, as well as Bayesian analyses were performed based on the morphological dataset. In maximum likelihood analysis (Fig. 1) *Europharinodes* was retrieved in a strongly supported (bootstrap value = 94) monophyletic Hybocephalini, as the basal-most group sister to its modern counterparts. In parsimony analysis the monophyly of Hybocephalini was recovered but with low support (bootstrap value < 50), and the position of *Europharinodes* was not solved. Nevertheless, neither the monophyly of Hybocephalini nor the position of *Europharinodes* were resolved in Bayesian analysis, in which the fossil was included in a clade (pp value = 0.69) comprising all modern hybocephalines and a lineage (pp value = 0.84) including *Caccoplectus* Sharp (Arhytodini), *Rhytus* Westwood (Arhytodini) and Clavigeritae. The unstable placement of *Europharinodes* in these analyses was likely a result rooted from the limited taxa sampling and character choice of the tribe and related groups, as all species of Hybocephalini are rarely represented in collections and are difficult to access. Morphologically, *Europharinodes* possesses most derived characters of modern Hybocephalini as currently defined (see Discussion section below), combined with the morphological evidence and the results of our phylogenetic analyses, the fossil is tentatively placed as a stem-group member of Hybocephalini.
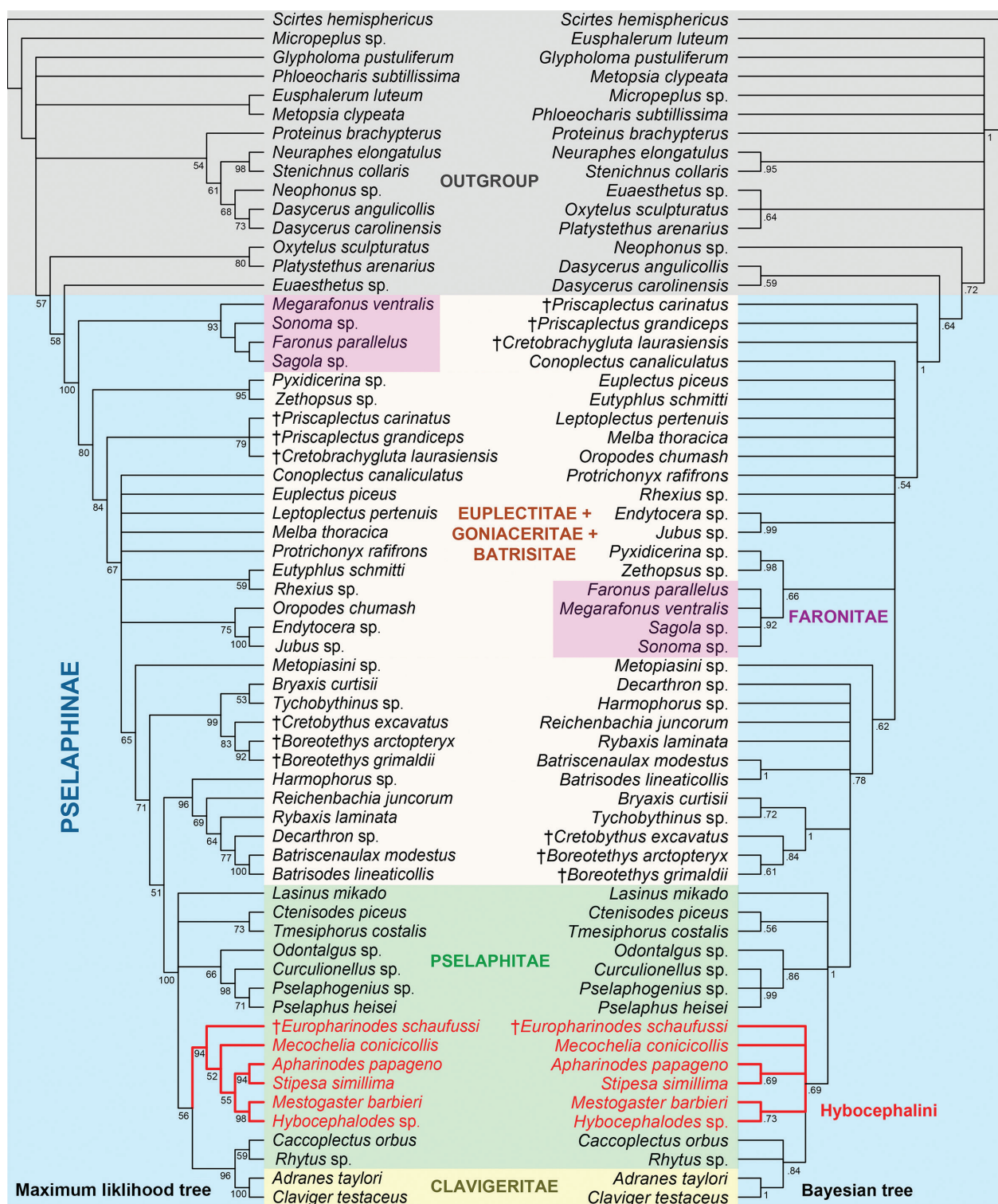
Figure 1. Maximum likelihood and Bayesian trees showing the placement of *Europharinodes schaufussi* **gen. et sp. nov.** Bootstrap values in maximum likelihood analysis and posterior probabilities in Bayesian analysis are annotated below each branch.

3.2. Systematic paleontology

Family Staphylinidae Latreille, 1802
Subfamily Pselaphinae Latreille, 1802
Tribe Hybocephalini Raffray, 1890

Europharinodes Yin & Cai gen. nov.

http://zoobank.org/0B631F8C-D490-4174-89F9-EE6274592F92

Figs 2–5

Type species. *Europharinodes schaufussi* **sp. nov.**

Diagnosis. Most of body covered with squamous setae; body generally compact; head, pronotum and femora coarsely punctate. Head roundly-triangular, with short and narrow frontal rostrum; large vertexal and frontal foveae present; antennal insertions close, antennomeres slightly elongate to sub-moniliform, clubs formed by apical three enlarged antennomeres; lacking ocular-mandibular carinae; clypeus sharply sloping, anterior margin carinate and rounded, lateral margins straight to eyes; maxillary palpi small, four-segmented, with short apical palpal cone. Pronotum with median and lateral antebasal foveae obscured by squamous setae; with antero-hypomeral foveae, lacking hypomeral carinae. Elytra each with two large basal foveae and two distinct discal striae. Each tarsus plesiomorphically with two subequal claws. Abdomen with tergite 1 (IV) slightly longer than 2 (V), tergites 1–4 (IV–VII) broadly sulcate at bases; paratergites moderately broad and laterally protruding. Aedeagus symmetrical, basal capsule enlarged, paired parameres elongate.

Description. Habitus (Figs 2B–D; 3A, B) stout, compact; most of body with squamous setae. Head (Fig. 3E) roundly triangular; vertex coarsely punctate, vertexal foveae (= dorsal tentorial pits; Fig. 3E; *vf*) relatively large, obscured by squamous setae; frontal fovea (Fig. 3E; *ff*) distinct, rostrum short and narrow, antennal insertions located at ventral surface of rostrum, tubercles barely raised; compound eyes (Fig. 3G; *ce*) large, prominent; lacking ocular-mandibular carina; clypeus (Fig. 3G; *cl*) sharply sloping, with broadly rounded, ridged anterior margin; labrum (Fig. 3G; *la*) transverse, subtrapezoidal; mandible (Fig. 3G; *ma*) with single distinct apical and preapical teeth; maxillary palpus small (Fig. 3H, I), four-segmented, with palpomere 1 small, indistinct, 2 (Fig. 3H; *p2*) pedunculate basally and broadened toward apex, 3 (Fig. 3H; *p3*) roundly triangular, 4 (Fig. 3H; *p4*) sub-fusiform, with short palpal cone at apex. Venter with small, widely separated gular foveae (= posterior tentorial pits; Fig. 3F; *gf*) in shared transverse impression, gular moderately raised along middle, weakly impressed admesally; neck region broad. Paired tentorial arms (Fig. 3E; *ta*) V-shaped, each branched at base and extending anteriorly to reach inner wall of clypeus (right arm broken at apex in holotype).

Pharynx (Fig. 3E; *ph*) about 2/3 of head length, posteriorly broadened. Antenna 11-segmented, moderately elongate, extending to approximately half of elytral length when extending posteriorly, antennomeres each slightly elongate to sub-moniliform, club (Fig. 3F) formed by enlarged apical three antennomeres.

Pronotum (Fig. 4A) approximately as long as broad, sides rounded, broadest at middle, anteriorly and posteriorly narrowed, surface with dense squamous setae (Fig. 3C); disc coarsely punctate, with squamous setae all over surface, covering median and lateral antebasal foveae (Fig. 4A, B; *maf*, *laf*), lacking sulcus or carina. Hypomeron extended, lacking carina, with anterior hypomeral fovea (Fig. 4B, C; *ahf*). Prosternum (Fig. 4C) with widely separated lateral procoxal foveae (Fig. 4C; *lpcf*), anterior part shorter than coxal part, margins of coxal cavity moderately carinate.

Elytra broadly truncate at bases, each elytron with two large basal foveae (Fig. 4D; *bef*), with two long discal striae (Fig. 4G; *ds*) extending from foveae to posterior elytral margin, lacking subhumeral fovea or marginal sulcus. Metathoracic (hind) wings (Fig. 2D; *hw*) fully developed.

Mesoventrite with median foveae (Fig. 4E; *mmsf*) originating from shared transverse impression, moderately separated, with pairs of large lateral and distinct anterolateral mesoventral foveae (not shown in figure); metaventrite with large, setose lateral coxal foveae (Fig. 4F; *lmcf*), with single median metaventral fovea (Fig. 4E; *mmtf*), posterior margin with small, narrow split at middle (Fig. 4E; *ms*); metacoxae broadly separated. Marginal carina of meso- and metaventrite complete (Fig. 4F; *mc*). Legs (Fig. 5A–C) moderately elongate; femora roughly punctate; with short tarsomere 1 and long tarsomere 2 and 3, 2 slightly longer than 3, each tarsus with two subequal pretarsal claws (Fig. 2G).

Abdomen constricted at base, with dense squamous setae (Fig. 3D); tergite 1 (IV) slightly longer than 2 (V), 2–4 (V–VII) subequal in length, tergites 1–4 (Fig. 4G, H; *t1–4*) each deeply and broadly sulcate at base, at lease with one pair of basolateral foveae (Fig. 4G; *blf*), tergite 5 (VIII) (Fig. 4H; *t5*) roundly triangular, transverse, medially roundly emarginate at posterior margin; sternite 2–5 (IV–VII) (Fig. 4H, I; *s2–5*) each broadly sulcate at base, with one pair of basolateral foveae (Fig. 3H; *blf*), 6 (VIII), sternite 6 (Fig. 4H, I; *s6*) transverse.

Males have modified sternites 4 and 5 (VI and VII). Aedeagus (Fig. 5D–F, I–K) dorso-ventrally symmetrical.

Etymology. The new generic name is a combination of Latin 'Eurōpa (Europe)' and genus *Apharinodes*, referring to the origin of the fossil in Baltic amber and its affinity with *Apharinodes*. The gender is feminine.

Europharinodes schaufussi Yin & Cai sp. nov.

http://zoobank.org/5BB9EDF8-BE3F-43D5-854B-89585BF7E453

Figs 2–6

Type material. Holotype (#SNUC-Paleo-0102), deposited in SNUC; a complete, well-preserved male in a 11.6 mm × 7.1 mm × 7.0 mm transparent yellow amber piece, without syninclusions; two surfaces regarding beetle's lateral and dorsal aspect were cut and polished for observation and photography.

Locality and horizon. Amber mined from the open-pit mine in Yantarny (Fig. 6), Kaliningrad region, Russia; layers between the Bartonian-Priabonian "Wilde Erde" plus "Blaue Erde" and the lower Lutetian "Untere Blaue Erde"; mid-Eocene, 45.0–38.0 Ma (Bukejs et al. 2019).

Diagnosis. As for the genus (*vide supra*), plus the following: body length approximately 2.1 mm; male antennae lacking modifications; sternites 4 and 5 each with a nodule at middle; aedeagus relatively stout, with short basoventral projection, median lobe with large basal capsule and dorsal diaphragm, sclerotized endophallus present, parameres elongate, each with two long setae at the apex.

Description. *Male.* Body (Figs 2B–D; 3A, B) length approximately 2.1 mm. Most surface of body covered with squamous setae. Head (Fig. 3E–G) roundly triangular, sub-rectangular at base, slightly longer than wide, length 0.47 mm, width across eyes 0.45 mm, length/width 1.04; vertex roughly punctate, almost flat, distinct vertexal foveae (dorsal tentorial pits) located above level of posterior margin of eyes; frons with narrow and short rostrum, anteriorly confluent with sharply declining clypeus, impressed between slightly raised antennal tubercles; clypeus with smooth surface, anterior margin broadly rounded, carinate and moderately raised; ocular-mandibular carina absent; postgenal region moderately projected. Venter with small, broadly separated gular foveae (posterior tentorial pits) in transverse impression, longitudinally ridged along middle, weakly impressed admesally. Compound eyes large and prominent, each composed of approximately 30 ommatidia, vertical length of eye/temple 2.1. Antenna moderately elongate, length 0.90 mm, lacking modification; antennomeres with rough surfaces; distinct club (Fig. 2B–D, F) formed by enlarged apical three antennomeres; antennomere 1 thick, subcylindrical, 2 and 3 each slightly elongate, 2 slightly longer and wider than 3, 4–7 subequal in width, approximately as long as wide, 8 shortest, slightly transverse, 9 enlarged, slightly longer than wide (including basal stalk), 10 as long as and slightly wider than 9, 11 largest, approximately as long as 9 and 10 combined, 1.24 times as broad as 10.

Prothorax with dense squamous setae (Fig. 3C). Pronotum (Fig. 4A) approximately as long as wide, length 0.42 mm, width 0.41 mm, length/width 1.02, widest at middle; sides rounded, convergent apically and basally; disc moderately convex; with distinct median and lateral antebasal foveae. Hypomeron confluent with prosternum, with antero-hypomeral fovea (Fig. 4B, C; *ahf*), lacking hypomeral ridge. Prosternum with anterior part much shorter than coxal part, with small, broadly separated lateral procoxal foveae (Fig. 4C; *lpcf*); margin of coxal cavity moderately carinate.

Elytra (Fig. 4D) with squamous setae finer than those of pronotum and abdomen, much wider than long, length 0.71 mm, width 0.90 mm, length/width 0.79 mm; each elytron with two large basal foveae and two distinct discal striae; humerus weakly prominent, lacking subhumeral fovea or marginal stria. Hindwing fully developed, membranous.

Mesoventrite short, well-demarcated from metaventrite; median mesoventral foveae (Fig. 4E; *mmsf*) moderately separated, with large lateral mesoventral fovea, mesoventral process short. Metaventrite distinctly raised admesally, inclined towards middle, with well-developed lateral mesocoxal (Fig. 4F; *lmcf*) and single median metaventral fovea (Fig. 4F; *mmtf*), posterior margin broadly emarginate, convex at middle, with small, short median split (Fig. 4F; *ms*).

Legs moderately elongate, lacking modification; mesotrochanter elongate; all femora coarsely punctate; tarsi with short tarsomeres 1 and long tarsomeres 2 and 3, with 3 slightly longer than 2; each tarsus with two sub-equal pretarsal claws (Fig. 2G).

Abdomen widest at lateral margins of paratergite 1 (IV), length 0.64 mm, width 0.66 mm; whole surface covered with broad squamous setae. Tergite 1 (IV) slightly longer than 2 (V), deeply and broadly sulcate at base, at least with one pair of basolateral foveae, lacking discal carina; tergite 2–4 (IV–VII) subequal in length along midline, each distinctly sulcate at base and with one pair of basolateral foveae (Fig. 4G; *blf*), tergite 5 (VIII) semicircular, transverse, posterior margin roundly emarginate at middle; accompanying paratergites 1–3 (Fig. 4G; *pt1–3*) broad, 4 triangular. Sternites successively shorter; sternites 2–5 (IV–VII) medially slightly impressed, each with broad sulcus at base and one pair of basolateral foveae (Fig. 4G; *blf*), lacking carina, 4 and 5 each with single nodule at middle (Fig. 4I; *mn*), sternite 6 (VIII) transverse, posterior margin broadly emarginate.

Aedeagus (Fig. 5D–F, I–K) 0.28 mm long, dorso-ventrally symmetrical, median lobe (Fig. 5E, J; *ml*) with large basal capsule (Fig. 5E, J; *bc*) and dorsal diaphragm (Fig. 5D, I; *dd*), narrowed towards apex and moderately bent ventrally, basoventral projection (Fig. 5E, J; *bp*) short; endophallus (Fig. 5G–J; *en*) well-sclerotized; parameres (Fig. 5E, J; *pa*) paired, elongate, rounded at apices, each with two long apical setae.

Female. Unknown.

Etymology. The new species is named after the German naturalist Ludwig W. Schaufuss (1833–1890), who described most of the known fossil psalaphines from Baltic amber.
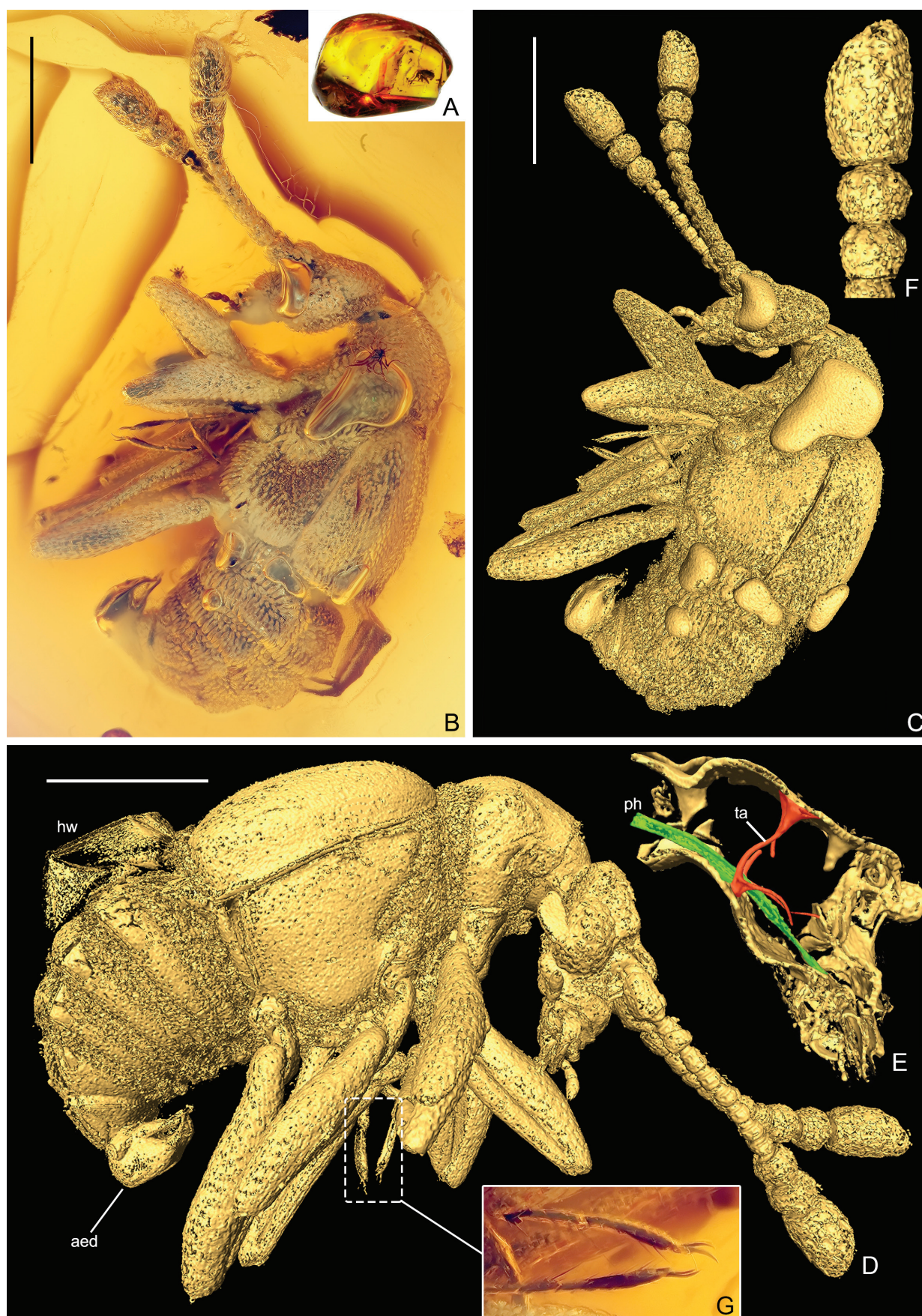
Figure 2. Amber piece (A) containing *Europharinodes schaufussi* **gen. et sp. nov.**, holotype, SNUC-Paleo-0102, and its morphological details (B–G) of (A, B, G: under incident light; C–F: X-ray microtomographic reconstruction). **A** Original amber piece containing the holotype before cutting and polishing. **B**, **C** Left lateral habitus. **D** Right lateral habitus. **E** Head in lateral view, show tentorial arms and pharynx. **F** Right antennal club. **G** Pro- and metatarsus and respective pretarsal claws. Abbreviations: aed, aedeagus; hw, hind wing; ph, pharynx; ta, tentorial arm. Scale bars: 0.5 mm in B–D, 0.2 mm in E, F.
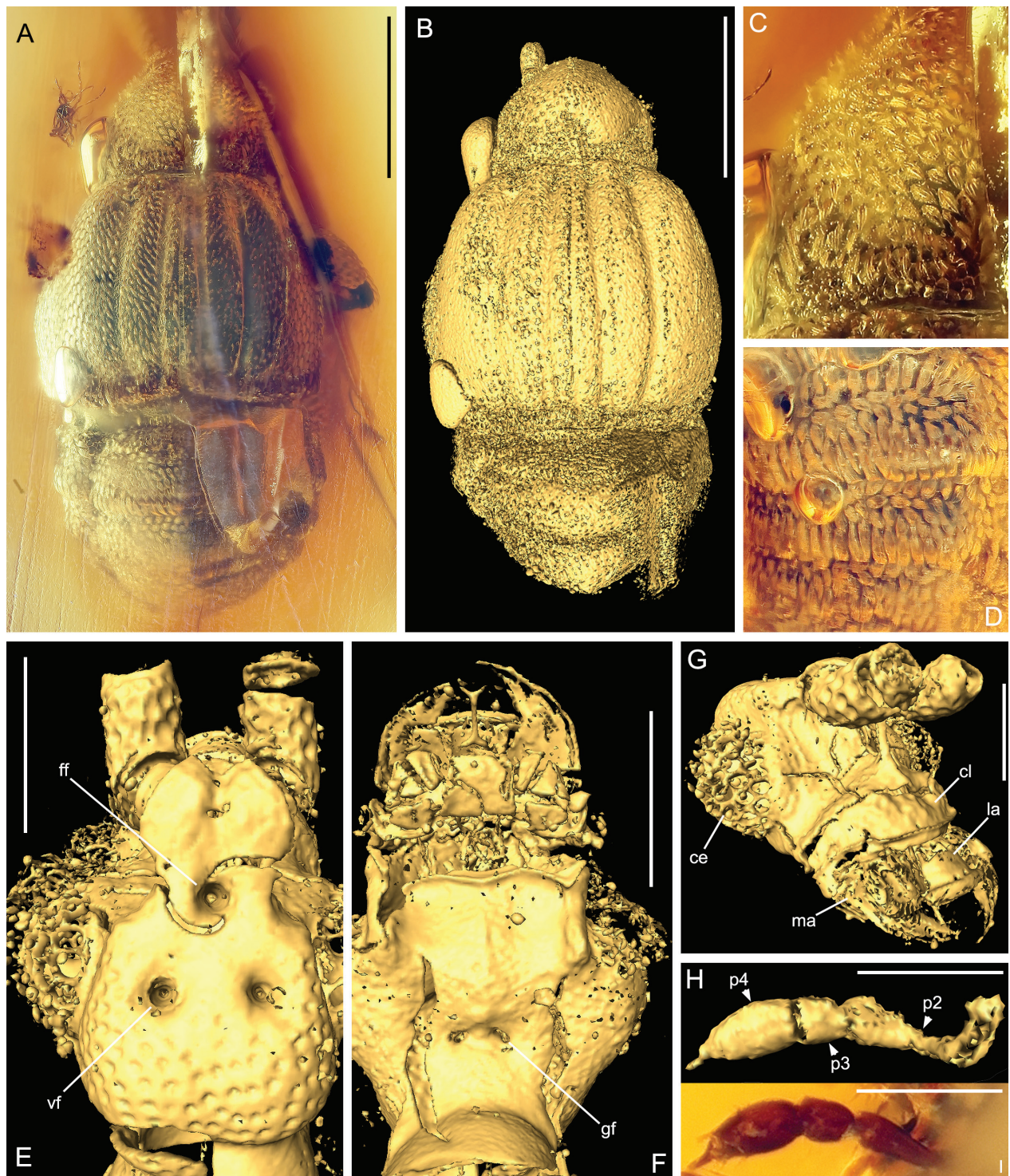
Figure 3. Morphology of *Europharinodes schaufussi* **gen. et sp. nov.**, holotype, SNUC-Paleo-0102 (A, C, D, I: under incident light; B, E–H: X-ray microtomographic reconstruction). **A**, **B** Dorsal habitus. **C** Left half of pronotum, showing squamous setae. **D** Lateral portion of the abdominal base, showing squamous setae. **E** Head dorsum. **F** Head venter. **G** Head, in antero-lateral view. **H**, **I** Left maxillary palpus. Abbreviations: ce, compound eye; cl, clypeus; ff, frontal fovea; gf, gular fovea; la, labrum; ma, mandible; p2–4, maxillary palpomere 2–4; vf, vertexal fovea. Scale bars: 0.5 mm in A, B, 0.2 mm in E–I.

4. Discussion

A monophyletic clade comprising the supertribes Pselaphitae and Clavigeritae was recovered in all analyses, with strong to moderate support (bootstrap value in ML tree = 100; pp value in MB tree = 1; bootstrap value in MP tree = 40) (Fig. 1, Supplementary material 3). Such a general relationship between these two higher groups was similarly recovered by previous studies focusing on different target groups (Parker 2016; Yin et al. 2017; Hlaváč et al. 2021) or based on different datasets (Jałoszyński
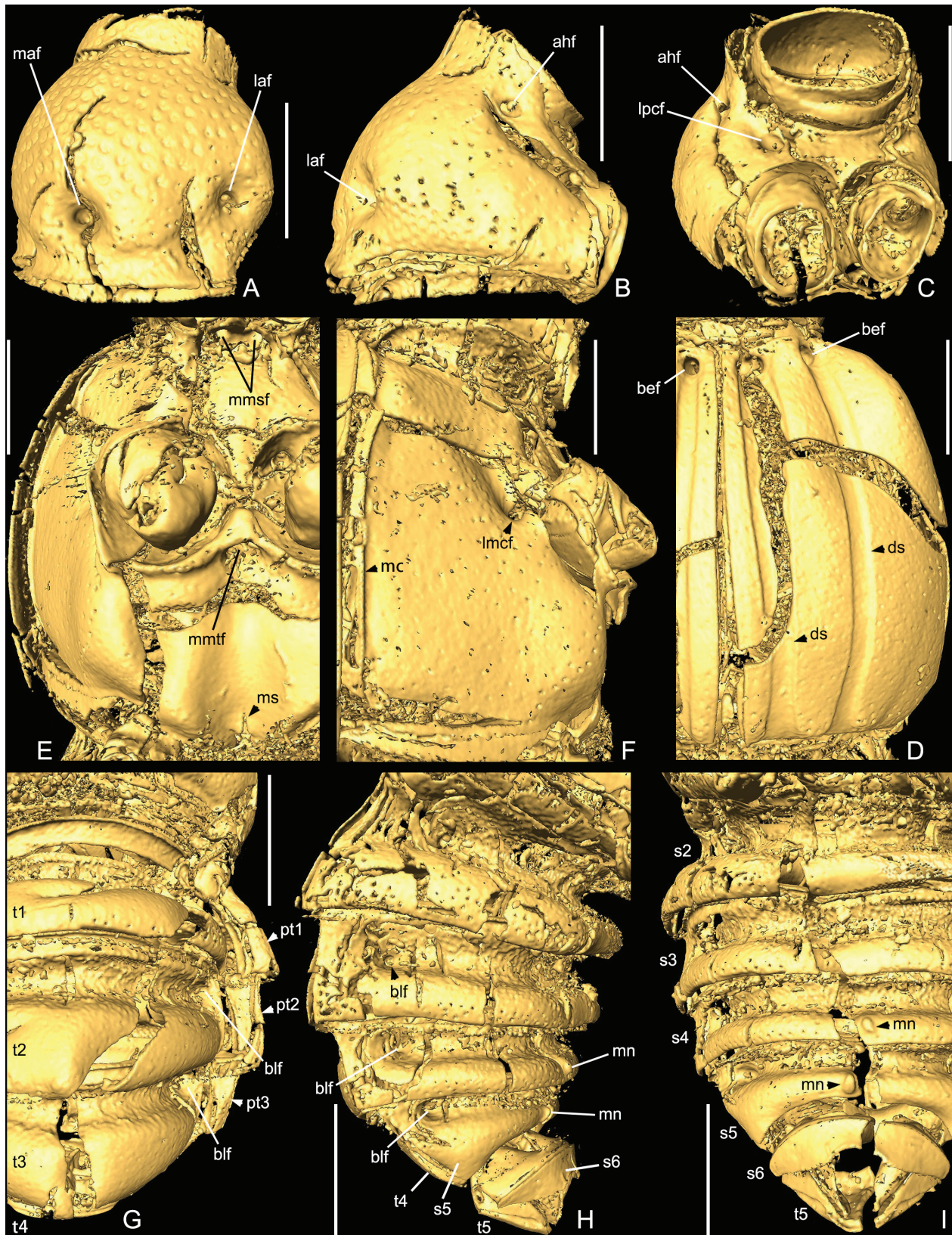
Figure 4. X-ray microtomographic reconstruction of *Europharinodes schaufussi* **gen. et sp. nov.**, holotype, SNUC-Paleo-0102. **A–C**: prothorax, dorsal (A), lateral (B) and ventral (C). **D** Right elytron. **E**, **F** Meso- and metathorax, ventral (E) and lateral (F). **G–I** Abdomen, dorsal (G), lateral (H) and ventral (I). Abbreviations: ahf, antero-hypomeral fovea; bef, basal elytral fovea; blf, basal lateral fovea; ds, discal stria; laf, lateral antebasal fovea; lmcf, lateral metaventral fovea; lpcf, lateral procoxal fovea; maf, median antebasal fovea; mmsf, median mesoventral fovea; mc, marginal carina; mmtf, median metaventral fovea; mn, median nodule; ms, median split; pt1–3, paratergite 1–3; s2–6, sternite 2–6 (IV–VIII); t1–5, tergite 1–5 (IV–VIII). Scale bars: 0.2 mm.

et al. 2022). Within the clade, the placement of *Europharinodes* varies in each analysis, likely due to limited taxa sampling and insufficient character selection. The strongest support was observed in the maximum likelihood tree (Fig.), in which a monophyletic Hybocephalini (bootstrap value = 94) was recovered as sister to a lineage composed of Arhytodini + Clavigeritae. *Europharinodes* was well-resolved as the basal-most group of the tribe, sister to all other modern hybocephalines. A similar topology from parsimonious analysis (Supplementary material 3) recovered a weakly supported monophyletic Hybocephalini (bootstrap value = 20), and *Europharinodes* was included in a probably soft polytomy. Neither the position of the fossil nor the monophyly of Hybocephalini were resolved in the Bayesian tree. The fossil was included in a weakly supported clade (pp value = 0.69) together with the other hybocephalines, *Caccoplectus*, *Rhytus*, and Clavigeritae.

Aside from the results inferred from phylogenetic analyses, the position of *Europharinodes* was indicated also by the fossil's unique combination of morphological traits. Within Pselaphinae the presence of squamous setae covering various parts of the body is a distinctive character state occurring in several tribes belonging to the supertribe Pselaphitae: Hybocephalini, Arhytodini, Ctenistini, Odontalgini, and Pselaphini. *Europharinodes* can be quickly ruled out from the latter three tribes by the small, reduced maxillary palpi that are only partially visible from the dorsal side. The members of Ctenistini often have maxillary palpomeres greatly extended laterally and with a distinct pencil-like apical projection (e.g., Li et al. 2021); Odontalgini is characterized by the long and basally pedunculate palpomeres 2 and 4, and a maximum number of foveae on the pronotum (Yin et al. 2016); and species of Pselaphini usually possess markedly extending palps that are often longer than the head and pronotum combined, and the squamous setae are usually confined to the basal impression of first visible tergite (Yin and Jiang 2016) (note: short maxillary palpi can be found in *Curculionellus* Westwood and a few more genera, but each genus is characteristic in the form of the palpi and other morphological characters). Both Hybocephalini and Arhytodini share the reduced size of maxillary palps, however, *Europharinodes* does not possess the derived characters that define Arhytodini: a) presence of ocular/gular-mandibular carinae; b) characteristic antennae modified in various forms, often greatly increased in length c) often enlarged eyes (normal size in *Sabarhytus* Löbl), d) femora and tibiae often with spines arranged in rows, e) variously modified tarsomeres, f) single pretarsal claws, and g) squamous setae usually confined to sulci, foveae, or articulations of body parts (Chandler and Wolda 1986; Chandler 1992, 2001; Löbl 2000).

Although the general morphology of *Europharinodes* is largely congruent with modern Hybocephalini (for tribal diagnosis see Chandler 2001: 495), the fossil exhibits a combination of characters found in different recent genera: heavy squamous setae that cover most areas of the body (Figs 2B, 3A, C, D) (*Apharinodes* Raffray), four-segmented maxillary palpi (Fig. 3H, I) (*Mestogas-ter* Schmidt-Göbel), antennal club formed by enlarged and unmodified three apical antennomeres (Fig. 2C, F) (*Hybocephalus* Motschulsky, *Hybocephalodes* Raffray, *Filigerinus* Jeannel, *Filigerodes* Jeannel, *Mestogaster*), projecting paratergites (Figs 3A, 4G) (*Mecochelia* Motschulsky), and visible tergites subequal in length along the midline (Figs 3A, 4G) (*Apharinodes*, *Filigerinus*, *Filigerodes*, *Mecochelia*, *Stipesa* Sharp) (Raffray 1890; Jeannel 1950, 1951; Nomura 1989; Chandler 2001; Yin and Jiang 2017). Other than a mosaic morphological combination, *Europharinodes* also possesses two presumably plesiomorphic characters which are unknown or rarely presented in modern species. The first is the presence of two subequal pretarsal claws on all tarsi (Fig. 2G), in contrast to one major anterior claw plus a reduced, posterior (accessary) claw in all extant species. The second, revealed by X-ray microtomography, is the dorso-ventrally symmetric aedeagus with an enlarged, bulbous basal capsule, a short, non-protruding endophallus, and large, elongate parameres. All extant members of Hybocephalini except for *Apharinodes* and a few *Stipesa* have a tubular aedeagus with a strongly constricted basal capsule (e.g., Jeannel 1950) similar to that of the genus *Pseudophanias* Raffray belonging to the tribe Tmesiphorini (Yin et al. 2015; Yin 2019; Inoue and Nomura 2020; Inoue et al. 2020); while *Apharinodes* has the aedeagus with a moderately bulbous basal capsule, but the endophallus is asymmetric and often protruding, and the parameres are short and reduced in size (Nomura 1989; Yin and Jiang 2017). Notably, *Europharinodes* bears a pair of antero-hypomeral foveae (Fig. 4B, C; *ahf*) on the prothorax, and a pair of anterolateral foveae (not shown in the figure) on the mesoventrite, two presumably autapomorphic characters that are absent among modern Hybocephalini but variously present in other pselaphine groups. *Europharinodes* also have more elongate, subquadrate antennomeres, opposed to the moderately to strongly transverse antennal segments in most extant species. The combination of the above morphological characters readily separates *Europharinodes* from all extant genera. Combining the morphological evidence and the results of our phylogenetic analyses present above, *Europharinodes* is tentatively postulated as a stem-group member of Hybocephalini.

For the first time, the endoskeletal structure of the head of a fossil Pselaphinae was partially reconstructed thanks to the application of X-ray microtomography technology. The tentorium (Fig. 2E; *ta*) of *Europharinodes* is more generalized and corresponds more to the ground plan of free-living groups such as Batrisitae (Nomura 1991b; Luo et al. 2021) than to Clavigeritae, of which the tentorium is distinctly reduced in size (Jałoszyński et al. 2020) as an adaptation to extreme myrmecophily. Surprisingly, the tentorium of *Europharinodes* shows a conspicuous difference from that of *Pselaphus heisei* Herbst (Pselaphitae: Pselaphini) which lacks anterior arms (Beutel et al. 2021). The dorsal tentorial arms of *Europharinodes* derived immediately from the inner wall of the large, distinct vertexal foveae (dorsal tentorial pits) (Fig. 3E; *vf*), and extending ventrally to connect posterior tentorial arms fusing with the inner wall of the widely separated

Figure 5. Morphology of *Europharinodes schaufussi* **gen. et sp. nov.**, holotype, SNUC-Paleo-0102 (A–H: X-ray microtomographic reconstruction; I–K: schematic). **A** Right foreleg. **B** Right middle leg. **C** Left hindleg. **D–F**, **I–K** Aedeagus, dorsal (D, I), lateral (E, J) and ventral (F, K). **G**, **H** endophallus, dorsal (G) and lateral (H). Abbreviations: bc, basal capsule; bp, basoventral projection; dd, dorsal diaphragm; en, endophallus; ml, median lobe; pa, paramere. Scale bars: 0.3 mm in A–C; 0.1 mm in D–K.
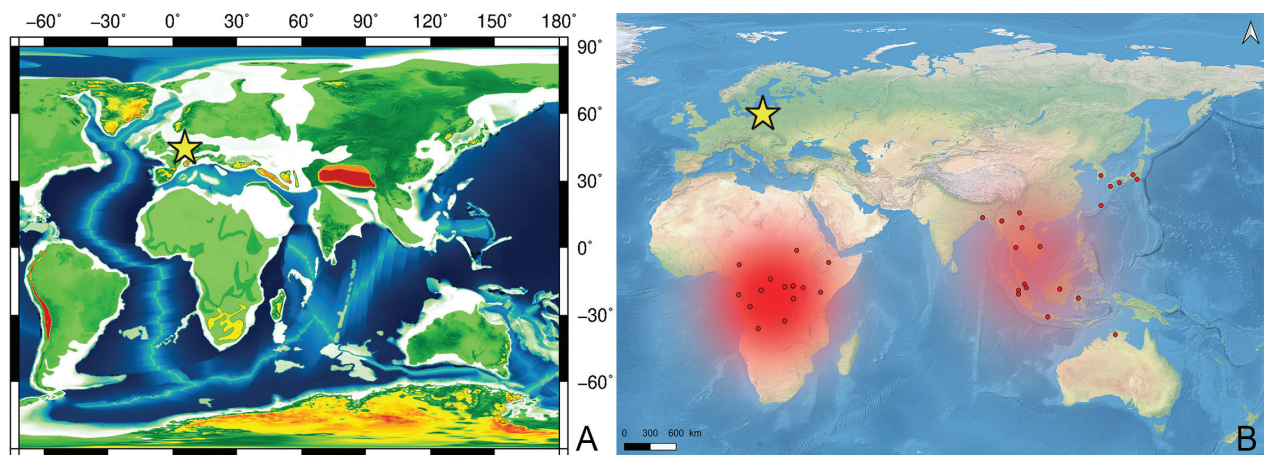
Figure 6. Distribution of Hybocephalini. **A:** Location of Baltic amber forest (yellow star) on a paleogeographic map of the middle Eocene. **B:** Distribution and species density of modern Hybocephalini (red dots) and location of Baltic amber deposit in the present-day Yantarny, Russia (yellow star).

gular foveae (posterior tentorial pits) (Fig. 3E; *gf*). The tentorium divergent anteriorly near the base of posterior arms to form curved and thin anterior arms, which extend anteriorly and end at the inner wall of the clypeus; the tentorial bridge is absent. Other inner structures of the head except for the pharynx cannot be clearly examined. The pharynx (Fig. 2E; *ph*) is the anterior-most part of the foregut (Beutel et al. 2013). In *Europharinodes* it extends from the anatomical mouth (which cannot be clearly seen) posteriorly to approximately the anterior 1/3 of prothoracic length. The posterior half of the pharynx is roughly the same width as the anterior half, and the pharyngeal lumen in cross-section appears to be suboval to slightly cordiform. The generalized pharynx, combined with the form of the mandibles, may indicate predacious habits of *Europharinodes*, albeit the biology of its modern relatives remains largely, if not at all, unknown. For the endoskeletal structures of the other main body segments, not much except for the three pairs of furcae can be observed. The profurcal arms are widely separated at the base, and in anterior view, each arm is slightly curved laterally. Only parts of the mesofurca and the basal part of the metafurca remain, but it would not be unreasonable to postulate that their overall morphology was generally concordant with that of modern Pselaphitae (e.g., Yin et al. 2013).

Different theories explaining the seemingly contradictory co-existence of thermophilic and temperate insect lineages in Baltic amber (Wheeler 1914), termed as the 'Wheeler's dilemma' (Archibald and Farrell 2003), have been proposed. Among them, the theory of an equable terrestrial palaeoclimate of the amber forest with temperate summer and mild winter of low-temperature seasonality (Archibald and Farrell 2003; Archibald et al. 2010) appears to be broadly favored by recent researchers (Wedmann et al. 2010; Perkovsky 2016; Alekseev 2017; Bogri et al. 2018; Schmidt et al. 2019), and corroborated by studies of floras (e.g., Sadowski et al. 2017). Here we adopt Archibald and Farrell (2003)'s explanation as the most convincing theory regarding the 'mixed' fauna from Baltic amber. On the other hand, discoveries of pres-

ent-day arthropod groups showing affinities with Afrotropical or Oriental regions in Baltic amber have been well-documented in published literature (e.g., Larsson 1978; Engel 2001), and a similar biogeographic connection also holds true for Hybocephalini. The present-day Hybocephalini are exclusively found in the Afrotropical and Australo-Oriental regions, with a higher species diversity occurring in sub-Saharan Africa (Fig. 6B). Notably, most species, if not all, are difficult to collect in the field and are rarely represented in museum collections. Insufficient available data, both morphological and molecular, prevented any meaningful studies tracing the origin and historical biogeography of this group. In this regard, the discovery of the first fossil member of the tribe is significant. The new fossil provides evidence that members of the stem-group Hybocephalini had already been well-established in Europe by the middle Eocene, which have since become extinct. During the Eocene–Oligocene transition, the global climate dramatically transformed from a 'greenhouse' to an 'icehouse' (Zachos et al. 2001; Hren et al. 2013), with an increase of seasonality (Eldrett et al. 2009; Mosbrugger et al. 2005; Utescher et al. 2015). Although dating the origin of Hybocephalini at this time appears to be premature due to the scarcity of paleontological data, this tribe may have been relatively widespread before the Eocene, and the northern Europe perhaps served as an important migration route for African-Asian spreading of the group. Following the Eocene–Oligocene Transition, the European representatives may have experienced significant declines in diversity and eventually become extinct, leaving the tropical survivors arriving in the Recent and forming isolated distributions as we observe today.

5.   Data availability

The original micro-CT data are available from the Zenodo repository (https://doi.org/10.5281/zenodo.6058375).

6. Competing interests

7. Acknowledgements

8. References

Alekseev VI (2017) Coleoptera from the middle-upper Eocene European ambers: generic composition, zoogeography and climatic implications. Zootaxa 4290: 401–443. https://doi.org/10.11646/zootaxa.4290.3.1

Archibald B, Bossert WH, Greenwood DR, Farrell BD (2010) Seasonality, the latitudinal gradient of diversity, and Eocene insects. Paleobiology 36 :374–398. https://doi.org/10.1666/09021.1

Archibald B, Farrell BD (2003) Wheeler's dilemma. Acta Zoologica Cracoviensia 46 (Supplement: Fossil Insects): 17–23.

Beutel RG, Friedrich F, Ge S-Q, Yang X-K (2013) Insect Morphology and Phylogeny. A Textbook for Students of Entomology. De Gruyter, Berlin, Boston, XV+516 pp. https://doi.org/10.1515/9783110264043

Beutel RG, Luo X-Z, Yavorskaya MI, Jałoszyński P (2021) Structural megadiversity in leaf litter predators – the head anatomy of *Pselaphus heisei* (Pselaphinae, Staphylinidae, Coleoptera). Arthropod Systematics & Phylogeny 79: 443–463. https://doi.org/10.3897/asp.79.e68352

Bogri A, Solodovnikov A, Żyła D (2018) Baltic amber impact on historical biogeography and palaeoclimate research: oriental rove beetle *Dysanabatium* found in the Eocene of Europe (Coleoptera, Staphylinidae, Paederinae). Papers in Palaeontology 4: 433–452. https://doi.org/10.1002/spp2.1113

Bukejs A, Alekseev VI, Pollock DA (2019) Waidelotinae, a new subfamily of Pyrochroidae (Coleoptera: Tenebrionoidea) from Baltic amber of the Sambian peninsula and the interpretation of Sambian amber stratigraphy, age and location. Zootaxa 4664: 261–273. https://doi.org/10.11646/zootaxa.4664.2.8

Chandler DS (1992) Short-winged mould beetles of the tribe Arhytodini of Panama, with descriptions of new taxa (Coleoptera: Pselaphidae: Pselaphinae), In: Quintero D, Aiello A (Eds). Insects of Panama and Mesoamerica: Selected Studies. Oxford University Press, Oxford, 339–344.

Chandler DS (2001) Biology, morphology, and systematics of the ant-like litter beetles of Australia (Coleoptera: Staphylinidae: Pselaphinae). Memoirs on Entomology International 15: 1–560.

Chandler DS, Wolda H (1986) Seasonality and diversity of *Caccoplectus*, with a review of the genus and description of a new genus, *Caccoplectinus* (Coleoptera: Pselaphidae). Zoologische Jahrbücher,

Abteilung für Systematik, Ökologie und Geographie der Tiere 113: 469–524.

Eldrett JS, Greenwood DR, Harding IC, Huber M (2009). Increased seasonality through the Eocene to Oligocene transition in northern high latitudes. Nature 459: 969–973. https://doi.org/10.1038/nature08069

Engel MS (2001) A monograph of the Baltic amber bees and evolution of the Apoidea (Hymenoptera). Bulletin of the American Museum of Natural History, 259: 1–192. https://doi.org/10.1206/0003-0090(2001)259<0001:AMOTBA>2.0.CO;2

Goloboff, P, Catalano, SA (2016) TNT version 1.5, including a full implementation of phylogenetic morphometrics. Cladistics: 32, 221–238. https://doi.org/10.1111/cla.12160

Hoang DT, Vinh LS, Flouri T, Stamatakis A, von Haeseler A, Minh BQ (2018) MPBoot: fast phylogenetic maximum parsimony tree inference and bootstrap approximation. BMC Evolutionary Biology 18: article 11. https://doi.org/10.1186/s12862-018-1131-3

Hlaváč P, Parker J, Maruyama M, Fikáček M (2021). Diversification of myrmecophilous Clavigeritae beetles (Coleoptera: Staphylinidae: Pselaphinae) and their radiation in New Caledonia. Systematic Entomology 46: 422–452. https://doi.org/10.1111/syen.12469

Hren MT, Sheldon ND, Grimes ST, Collinson ME, Hooker JJ, Bugler M, Lohmann KC (2013) Terrestrial cooling in Northern Europe during the Eocene–Oligocene transition. Proceedings of the National Academy of Sciences of the United States of America 110: 7562–7567. https://doi.org/10.1073/pnas.1210930110

Inoue S, Nomura S (2020) A new species of the genus *Pseudophanias* Raffray, 1890 from Thailand (Coleoptera: Staphylinidae: Pselaphinae). Japanese Journal of Systematic Entomology 26: 336–339.

Inoue S, Nomura S, Yin Z-W (2020) Three new species of *Pseudophanias* Raffray from Japan and Taiwan Island, and synonymy of *Chandleriella* Hlaváč with *Pseudophanias* (Coleoptera, Staphylinidae, Pselaphinae). ZooKeys 987: 135–156. https://doi.org/10.3897/zookeys.987.53648

Jałoszyński P, Luo X-Z, Beutel RG (2020) Profound head modifications in *Claviger testaceus* (Pselaphinae, Staphylinidae, Coleoptera) facilitate integration into communities of ants. Journal of Morphology 281: 1072–1085. https://doi.org/10.1002/jmor.21232

Jałoszyński P, Luo X-Z, Beutel RG (2022) Evolution of cephalic structures in extreme myrmecophiles: a lesson from Clavigeritae (Coleoptera: Staphylinidae: Pselaphinae). Cladistics (2022): 1–24 (early view). https://doi.org/10.1111/cla.12498

Jeannel R (1950) Faune du Congo Belge et du Ruanda Urundi, II: Pselaphidae. Annales du Musée du Congo Belge, Tervuren (Série 8°: Sciences Zoologiques) 2: 1–275.

Jeannel R (1951) Psélaphides de l'Angola (Coléoptères) recueillis par M. A. de Barros Machado. Publicações Culturais da Companhia de Diamantes de Angola No. 9, 125 pp.

Kalyaanamoorthy S, Minh BQ, Wong TKF, von Haeseler A, Jermiin LS (2017) ModelFinder: fast model selection for accurate phylogenetic estimates. Nature Methods 14: 587–589. https://doi.org/10.1038/nmeth.4285

Lewis PO (2001) A likelihood approach to estimating phylogeny from discrete morphological character data. Systematic Biology 50: 913–925. https://doi.org/10.1080/106351501753462876

Li Q-Q, Wang Y, Yin Z-W (2021) First species of *Ctenisomorphus* Raffray, 1890 from China, with comments on *Largeyeus* J.-K. Li, 1993 (Coleoptera, Staphylinidae, Pselaphinae). Zootaxa 5016: 588–596. https://doi.org/10.11646/zootaxa.5016.4.9

Li Y-D, Tihelka E, Liu Z-H, Huang D-Y, Cai C-Y. New mid-Cretaceous cryptic slime mold beetles and the early evolution of Sphindidae

(Coleoptera: Cucujoidea). Arthropod Systematics & Phylogeny 79: 587–597. https://doi.org/10.3897/asp.79.e72724

Löbl I (2000) *Pachacuti chandleri* sp. n. and *Sabarhytus kinabalu* gen. et sp. n. with comments on Arhytodini and Pselaphini (Coleoptera, Staphylinidae, Pselaphinae). Biologia, Bratislava 55: 143–149.

Löbl I, Kurbatov SA (2001) The Batrisini of Sri Lanka (Coleoptera: Staphylinidae: Pselaphinae). Revue Suisse de Zoologie 108: 559–697. https://doi.org/10.5962/bhl.part.80163

Larsson SG (1978) Baltic amber: A Palaeobiological Study. Scandinavian Science Press, Klampenborg, 192 pp.

Luo X-Z, Hlaváč P, Jałoszyński P, Beutel RG (2021) In the twilight zone—The head morphology of *Bergrothia saulcyi* (Pselaphinae, Staphylinidae, Coleoptera), a beetle with adaptations to endogean life but living in leaf litter. Journal of Morphology 282: 1170–1187. https://doi.org/10.1002/jmor.21361

Mosbrugger V, Utescher T, Dilcher DL. 2005. Cenozoic continental climatic evolution of Central Europe. Proceedings of the National Academy of Sciences of the United States of America 102: 14964–14969. https://doi.org/10.1073/pnas.0505267102

Newton AF (2018) Staphyliniformia world catalog database. In: Bánki O, Roskov Y, Döring M, Ower G, Vandepitte L, Hobern D, Remsen D, Schalk P, DeWalt RE, Keping M, Miller J, Orrell T, Aalbu R, Adlard R, Adriaenssens E, Aedo C, Aescht E, Akkari N, Alonso-Zarazaga MA et al. Catalogue of Life Checklist (Nov. 2018). Available from https://www.catalogueoflife.org/data/dataset/1204 (Accessed 18 February 2020)

Newton AF, Chandler DS (1989) World catalog of the genera of Pselaphidae (Coleoptera). Fieldiana, Zoology (New Series) 53: 1–93. https://doi.org/10.5962/bhl.title.3209

Newton AF, Thayer MK (1995) Protopselaphinae new subfamily for *Protopselaphus* new genus from Malaysia, with a phylogenetic analysis and review of the Omaliine Group of Staphylinidae including Pselaphidae (Coleoptera). In: Pakaluk J, Ślipiński SA (Eds) Biology, Phylogeny, and Classification of Coleoptera: Papers Celebrating the 80th Birthday of Roy A. Crowson, Muzeum i Instytut Zoologii PAN, Warszawa, 219–320.

Nguyen LT, Schmidt HA, von Haeseler A, Minh BQ (2015) IQ-TREE: A fast and effective stochastic algorithm for estimating maximum likelihood phylogenies. Molecular Biology and Evolution 32: 268–274. https://doi.org/10.1093/molbev/msu300

Nixon KC (2002) WinClada (Beta), V. 1.00.08 Software Published by the Author, Ithaca, New York (online) [WWW document]. URL http://www.cladistics.com (program downloaded on 5th Dec. 2003).

Nomura S (1989) Description of a new species of *Apharinodes* (Coleoptera, Pselaphidae) from Okinawa Island, Japan. Japanese Journal of Entomology 57: 278–282.

Nomura S (1991a) Crisis of *Apharinodes papageno* (Pselaphidae) at the type locality in Okinawa Island, Southwest Japan. Elytra 19: 84 (in Japanese).

Nomura S (1991b) Systematic study on the genus *Batrisoplisus* and its allied genera from Japan (Coleoptera, Pselaphidae). Esakia 30: 1–462.

Parker J (2016) Emergence of a superradiation: pselaphine rove beetles in mid-Cretaceous amber from Myanmar and their evolutionary implications. Systematic Entomology 41: 541–566. https://doi.org/10.1111/syen.12173

Parker J, Grimaldi DA (2014) Specialized myrmecophily at the ecological dawn of modern ants. Current Biology 24: 2428–2434. https://doi.org/10.1016/j.cub.2014.08.068

Perkovsky EE (2016) Tropical and Holarctic ants in late Eocene ambers. Vestnik Zoologii 50: 111–122. http://dx.doi.org/10.1515/vzoo-2016-0014

Poblete F, Dupont-Nivet G, Licht A, van Hinsbergen DJJ, Roperch P, Mihalynuk MG, Johnston ST, Guillocheau F, Baby G, Fluteau F, Robin C, van der Linden TJM, Ruiz D, Baatsen MLJ (2021) Towards interactive global paleogeographic maps, new reconstructions at 60, 40 and 20 Ma. Earth-Science Reviews 214: 103508. https://doi.org/10.1016/j.earscirev.2021.103508

Raffray A (1890) Étude sur les Psélaphides. V. Tableaux synoptiques. – Notes et synonymie. Revue d'Entomologie 9: 81–172.

Rambaut A, Drummond AJ, Xie D, Baele G, Suchard MA (2018) Posterior summarisation in Bayesian phylogenetics using Tracer 1.7. Systematic Biology 67: 901–904. https://doi.org/10.1093/sysbio/syy032

Ronquist F, Teslenko M, Mark P. van der Ayres DL, Darling A, Höhna S, Larget B, Liu L, Suchard MA, Huelsenbeck JP (2012) MrBayes 3.2: Efficient Bayesian phylogenetic inference and model choice across a large model space. Systematic Biology 61: 539–542. https://doi.org/10.1093/sysbio/sys029

Ross AJ (2019) Burmese (Myanmar) amber checklist and bibliography 2018. Palaeoentomology 2: 22–84. https://doi.org/10.11646/palaeoentomology.2.1.5

Ross AJ (2020) Supplement to the Burmese (Myanmar) amber checklist and bibliography, 2019. Palaeoentomology 3: 103–118. https://doi.org/10.11646/palaeoentomology.3.1.14

Ross AJ (2021) Supplement to the Burmese (Myanmar) amber checklist and bibliography, 2020. Palaeoentomology 4: 57–76. https://doi.org/10.11646/palaeoentomology.4.1.11

Rust J, Singh H, Rana RS, McCann T, Singh L, Anderson K, Sarkar, Nascimbene PC, Stebner F, Thomas JC, Kraemer MS, Williams CJ, Engel MS, Sahni A, Grimaldi D (2010) Biogeographic and evolutionary implications of a diverse paleobiota in amber from the early Eocene of India. Proceedings of the National Academy of Sciences of the United States of America 107: 18360–18365. https://doi.org/10.1073/pnas.1007407107

Sadowski E-M, Schmidt AR, Seyfullah LJ, Kunzmann L (2017) Conifers of the 'Baltic amber forest' and their palaeoecological significance. Land Oberösterreich, Oberösterreichisches Landesmuseum, Linz, Austria, 73 pp.

Schmidt J, Scholz S, Kavanaugh DH (2019) Unexpected findings in the Eocene Baltic amber forests: Ground beetle fossils of the tribe Nebriini (Coleoptera: Carabidae). Zootaxa 4701: 350–370. https://doi.org/10.11646/zootaxa.4701.4.2

Schaufuss LW (1890) System-schema der Pselaphiden, ein Blick in die Vorzeit, in die Gegenwart und in die Zukunft. Tijdschrift voor Entomologie 33: 101–162.

Shin S, Clarke DJ, Lemmon AR, Lemmon EM, Aitken AL, Haddad S, Farrell BD, Marvaldi AE, Oberprieler RG, McKenna DD (2017) Phylogenomic data yield new and robust insights into the phylogeny and evolution of weevils. Molecular Biology and Evolution 35: 823–836. https://doi.org/10.1093/molbev/msx324

Shorthouse D.P. (2010) SimpleMappr, an online tool to produce publication-quality point maps. Available from https://www.simplemappr.net. (Accessed 22 February 2022)

Spahr U (1981) Systematischer Katalog der Bernstein- und Kopal-Käfer (Coleoptera). Stuttgarter Beiträge zur Naturkunde, Serie B (Geologie und Paläontologie) 80: 1–107.

Sugaya H (2003) Notes on *Apharinodes papageno* (Coleoptera, Staphylinidae, Pselaphinae) in Okinawa-jima, the Ryukyus, Japan. Elytra 31: 125–126.

Utescher T, Bondarenko OV, Mosbrugger V (2015) The Cenozoic Cooling – continental signals from the Atlantic and Pacific side of Eurasia. Earth and Planetary Science Letters 415: 121–133. https://doi.org/10.1016/j.epsl.2015.01.019

Wheeler WM (1914) The Ants of the Baltic Amber. Schriften der Physikalisch-ökonomischen Gesellschaft zu Königsberg 55: 1–142. https://doi.org/10.5962/bhl.title.14207

Wedmann S, Poschmann M, Hörnschemeyer T (2010) Fossil insects from the Late Oligocene Enspel Lagerstätte and their palaeobiogeographic and palaeoclimatic significance. Palaeobiodiversity and Palaeoenvironments 90: 49–58. https://doi.org/10.1007/s12549-009-0013-5

Weitschat W, Wichard W (2010) Baltic amber. In: Penney D (Ed) Biodiversity of Fossils in Amber from the Major World Deposits. Manchester, UK: Siri Scientific Press, 80–115.

Yang Z (1994) Maximum likelihood phylogenetic estimation from DNA sequences with variable rates over sites: Approximate methods. Journal of Molecular Evolution 39: 306–314. https://doi.org/10.1007/BF00160154

Yin Z-W (2019) First record of the genus *Chandleriella* Hlaváč (Coleoptera: Staphylinidae: Pselaphinae) from China, with description of a second species. Zootaxa 4571: 432–438.

Yin Z-W (2022) The Batrisini of Tibet: unveiling an enigmatic ant-loving beetle diversity at Earth's "Third Pole" (Coleoptera, Staphylinidae, Pselaphinae). Zootaxa 5111: 1–211. accepted manuscript. https://doi.org/10.11646/zootaxa.5111.1.1

Yin Z-W, Cai C-Y (2021) A new Brachyglutini from mid-Cretaceous amber of northern Myanmar (Coleoptera: Staphylinidae: Pselaphinae). Cretaceous Research 124: 104807. https://doi.org/10.1016/j.cretres.2021.104807

Yin Z-W, Chandler DS, Cai C-Y (2019b) *Priscaplectus* gen. nov. and two new species in mid-Cretaceous amber from Myanmar (Coleoptera: Staphylinidae: Pselaphinae). Cretaceous Research 103: 104174. https://doi.org/10.1016/j.cretres.2019.07.004

Yin Z-W, Coulon G, Bekchiev R (2015) A new species of *Pseudophanias* Raffray from a cave in central Nepal (Coleoptera: Staphylinidae: Pselaphinae). Zootaxa 4048: 446–450. https://doi.org/10.11646/zootaxa.4048.3.10

Yin Z-W, Jiang R-X (2016) Taxonomic notes on the genus *Bellenden* Chandler (Coleoptera, Staphylinidae, Pselaphinae). ZooKeys 638: 27–32. https://doi.org/10.3897/zookeys.638.10958

Yin Z-W, Jiang R-X (2017) *Apharinodes sinensis* sp. n. (Coleoptera: Staphylinidae: Pselaphinae) from China, and discovery of male wing dimorphism in Hybocephalini. Revue suisse de Zoologie 124: 9–14. https://doi.org/10.5281/zenodo.322660

Yin Z-W, Kurbatov S, Cuccodoro G, Cai C-Y (2019a) *Cretobrachygluta* gen. nov., the first and oldest Brachyglutini in mid-Cretaceous amber from Myanmar (Coleoptera: Staphylinidae: Pselaphinae). Acta Entomologica Musei Nationalis Pragae 59: 101–106. https://doi.org/10.2478/aemnp-2019-0008

Yin Z-W, Lü L, Yamamoto S, Thayer MK, Newton AF, Cai C-Y (2020) Dasycerine rove beetles: Cretaceous diversification, phylogeny and historical biogeography (Coleoptera: Staphylinidae: Dasycerinae). Cladistics 37 (2021): 185–210. https://doi.org/10.1111/cla.12430

Yin Z-W, Newton AF, Zhao TX (2016) *Odontalgus dongbaiensis* sp. n. from eastern China, and a world catalog of Odontalgini (Coleoptera: Staphylinidae: Pselaphinae). Zootaxa 4117: 567–579. https://doi.org/10.11646/zootaxa.4117.4.8

Yin Z-W, Nomura S, Li L-Z (2013) Redescription of *Tyrus* Aubé and *T. sinensis* Raffray (Coleoptera: Staphylinidae: Pselaphinae), and two new species from Sichuan, Southwest China. Zootaxa 3637: 47–57. https://doi.org/10.11646/zootaxa.3637.1.5

Yin Z-W, Parker J, Cai C-Y, Huang D-Y, Li L-Z (2017). A new stem bythinine in Cretaceous Burmese amber and early evolution of specialized predatory behaviour in pselaphine rove beetles (Coleoptera: Staphylinidae). Journal of Systematic Palaeontology 16 (2018): 531–541. https://doi.org/10.1080/14772019.2017.1313790

Yin Z-W, Zhao Q-H, Cai C-Y (2021) *Megabythinus* gen. nov., a new stem-group Pselaphinae from mid-Cretaceous Myanmar amber (Coleoptera, Staphylinidae). Cretaceous Research 125: 104879. https://doi.org/10.1016/j.cretres.2021.104879

Zachos J, Pagani M, Sloan L, Thomas E, Billups K (2001) Trends, rhythms, and aberrations in global climate 65 Ma to present. Science 292: 686–693. https://doi.org/10.1126/science.1059412

Supplementary material 1

Characters and character states

Authors: Yin et. al (2022)
Data type: .docx
Explanation note: List of morphological characters and character states used in phylogenetic analyses (adapted from Parker 2016; Yin et al. 2017, 2019b).
Copyright notice: This dataset is made available under the Open Database License (http://opendatacommons.org/licenses/odbl/1.0). The Open Database License (ODbL) is a license agreement intended to allow users to freely share, modify, and use this Dataset while maintaining this same freedom for others, provided that the original source and author(s) are credited.
Link: https://doi.org/10.3897/asp.80.e82644.suppl1

Supplementary material 2

Morphological dataset

Authors: Yin et. al (2022)
Data type: .nex
Explanation note: Morphological dataset used for the analyses.
Copyright notice: This dataset is made available under the Open Database License (http://opendatacommons.org/licenses/odbl/1.0). The Open Database License (ODbL) is a license agreement intended to allow users to freely share, modify, and use this Dataset while maintaining this same freedom for others, provided that the original source and author(s) are credited.
Link: https://doi.org/10.3897/asp.80.e82644.suppl2

Supplementary material 3

Results of the maximum parsimony analyses

Authors: Yin et. al (2022)
Data type: .tif
Explanation note: Fifty percent majority-rule consensus cladogram of 4400 most parsimonious trees obtained by the 'Traditional search' analysis of a data matrix of unordered adult morphological characters under implied weighting (K = 3; tree length = 173; consistency index = 0.34; retention index = 0.82), showing placement of *Europharinodes schaufussi* gen. & sp. n. Standard Bootstrap ($\geq$ 50) are shown below branches. Unambiguously optimized character changes are plotted along internodes. Black circles indicate unique character changes; white circles indicate parallelisms or reversals; character numbers and states are shown above and below circles, respectively.
Copyright notice: This dataset is made available under the Open Database License (http://opendatacommons.org/licenses/odbl/1.0). The Open Database License (ODbL) is a license agreement intended to allow users to freely share, modify, and use this Dataset while maintaining this same freedom for others, provided that the original source and author(s) are credited.
Link: https://doi.org/10.3897/asp.80.e82644.suppl3